Supplementary Figure

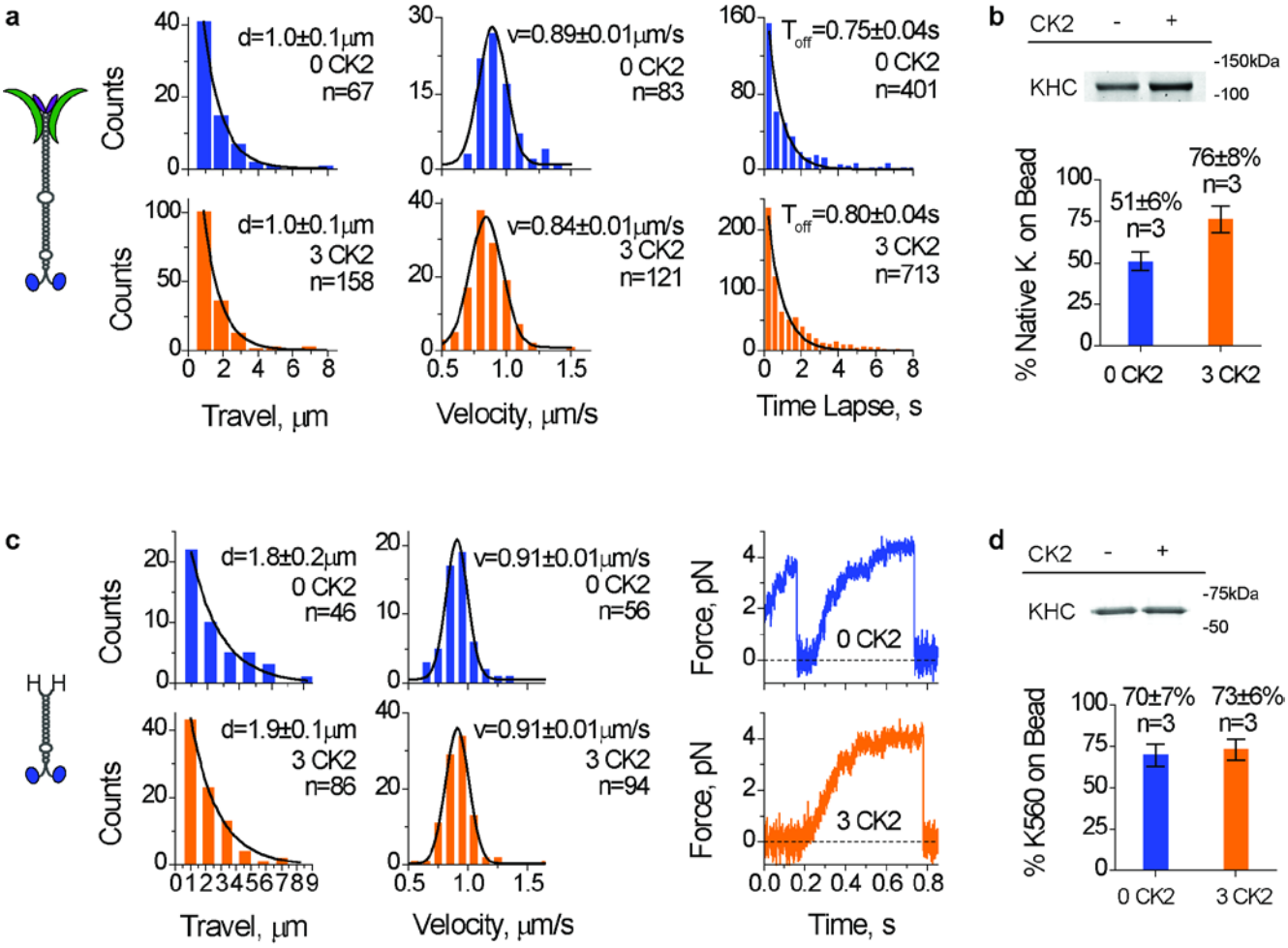

Supplementary Figure S1. Effect of CK2 treatment on the single motor function of active kinesin, and motor:bead recruitment. Native or truncated kinesins were incubated with or without CK2 for 40 at 30°C prior to functional studies. '3 CK2' indicates an incubation ratio of 3 kinase molecules per motor. '0 CK2' indicates CK2-blank samples. (**a**) Distributions of travel distance, velocity, and time lapse for beads carried by single native kinesins. 'Time lapse' denotes the time interval between consecutive binding events when a bead, carried by a single active kinesin, was spatially confined to the vicinity of a microtubule. CK2-treated kinesin (orange) required significantly more dilution relative to the untreated kinesin (blue) to reach the single motor range (~ 30% binding fraction[11]). (**b**) Effect of CK2 treatment (3:1 CK2:motor) on motor-bead association for the native kinesin, assayed by Coomassie

stain. Carboxylated polystyrene beads were used to evaluate non-specific binding between the native kinesin and the bead. Values shown were determined as the fraction of bead-bound motors *vs.* total input amount (mean ± SEM, n = 3 each). (**c**) Distributions of travel distance and velocity, and representative force traces of beads carried by a single K560 (~ 30% binding fraction). CK2-treated K560 again required significantly more dilution relative to the untreated sample to reach the single motor range. (**d**) Effect of CK2 on K560-bead association, assayed by Krypton IR stain (Thermal Scientific). Carboxylated polystyrene beads were used to evaluate non-specific binding between K560 and the bead (Supplementary Methods). Values shown were determined as the fraction of bead-bound motors *vs.* total input amount (mean ± SEM, n = 3 each).

Supplementary Table S1

	Accession Number	Unique Peptides		% Coverage		Protein Name
		Exp. 1	Exp. 2	Exp. 1	Exp. 2	
K560	P33176	61	49	47.7	42.9	Kinesin-1 heavy chain
	Q86YZ3	1	n/a	0.6	n/a	Hornerin
	P07900	1	n/a	1.5	n/a	Heat shock protein HSP 90-alpha
	P68400	1	n/a	4.6	n/a	Casein kinase II subunit alpha
K560+CK2	P33176	57	73	47.0	51.1	Kinesin-1 heavy chain
	P68400	37	32	72.1	67.8	Casein kinase II subunits alpha
	P67870	24	22	88.4	71.6	Casein kinase II subunits beta
	P11021	1	n/a	2.4	n/a	78 kDa glucose-regulated protein
	Q5H9R7	1	n/a	1.5	n/a	Serine/threonine-protein phosphatase 6 regulatory subunit 3

Table S1. Purity of K560 and CK2 samples examined via liquid chromatography-mass spectrometry. Two independent experiments were carried out for K560, and K560+CK2. No significant contamination was detected for either CK2 or K560. The potential contaminants were not meaningful: they were identified by only one unique peptide each (with less than 4.5% sequence coverage), and were detected in only one of the two parallel experiments. Tubulin β and α isoforms associated with the final microtubule affinity step in K560 purification[22] (Fig. 2b), were present in both K560 and K560+CK2 samples, and are not included in this table. Activation of kinesin (native or truncated) was independently verified using this particular CK2 lot; the same magnitude of activation was observed across three different lots of CK2 used in the current study.

Supplementary Table S2

(i)	TKEYELLS(Phospho)DELNQK+2
m/z	Ion
275.136	y2(-0.035)
341.173	b3-H2O(-0.0089)
359.102	b3(-0.091)
372.136	y3-NH3(-0.052)
389.183	y3(-0.031)
502.211	y4(-0.087)
522.322	b4(0.066)
580.328	b9+2(0.078)
613.347	y5-H2O(0.017)
631.312	y5(-0.029)
651.254	b5(-0.044)
693.325	b11-NH3+2(0.53)
746.35	y6(-0.018)
764.27	b6(-0.11)
815.27	y7-H3PO4(-0.12)
847.096	MH-H3PO4+2(0.67)
877.352	b7(-0.11)
896.408	y7-NH3(0.068)
913.227	y7(-0.14)
928.303	y8-H3PO4(-0.17)
1041.328	y9-H3PO4(-0.23)
1061.167	b9-H3PO4(-0.35)
1139.388	y9(-0.15)
1159.345	b9(-0.15)
1303.443	b11-H3PO4(-0.20)
1401.615	b11(-0.0035)
1431.54	y11(-0.10)

(ii)	TKEYELLSDELNQK+2
m/z	Ion
258.218	y2-NH3(0.073)
275.188	y2(0.017)
341.293	b3-H2O(0.11)
359.267	b3(0.074)
372.235	y3-NH3(0.047)
389.242	y3(0.028)
485.262	y4-NH3(-0.0098)
502.187	y4(-0.11)
516.784	b4(-0.062)
614.262	y5-NH3(-0.052)
631.284	y5(-0.057)
651.256	b5(-0.042)
746.349	y6(-0.019)
764.237	b6(-0.15)
816.373	y7-NH3(-3.9e-4)
833.385	y7(-0.015)
846.728	MH-NH3+2(-0.19)
859.285	b7-H2O(-0.17)
877.407	b7(-0.060)
946.344	y8(-0.14)
964.393	b8(-0.11)
1059.489	y9(-0.079)
1079.324	b9(-0.20)
1188.499	y10(-0.11)
1208.521	b10(-0.047)
1321.586	b11(-0.066)
1351.665	y11(-0.0090)
1435.595	b12(-0.10)
1480.668	y12(-0.049)
1563.783	b13(0.029)

Table S2. Corresponding m/z values of each y- and b- ions for LC-MS/MS spectra (Fig. 3d) of tryptic phosphopeptide (**i**, TKEYELLS(phospho)DELNQK) and non-phosphopeptide (**ii**, TKEYELLSDELNQK). m/z values are highlighted in black. b-ions are highlighted in red, with mass errors for the assigned ion types in parenthesis.

Supplementary Discussion

Binding fraction measurements detect/reflect the presence of active motors.

In binding fraction measurements, beads were held by the optical trap in the vicinity of a microtubule for 30 seconds, and binding events were scored only if the bead bound to, and processed along the microtubule. A wait time of 30 sec is sufficient for binding if there is any active kinesin present. Kinesin's on-rate when confined to the vicinity of a microtubule is typically 2-5 per second[44], allowing repeated opportunities for the motor to bind in this trial time. Svoboda and Block[11] demonstrated that the probability of a bead binding/moving along the microtubule is negligible in repeated trials if the bead failed to bind and move in the first trial. We obtained similar results when we extended the wait time from 30 to 120 sec. Here the overall binding fraction of untreated kinesin was kept below 30%, and no more than 2% of moving beads were simultaneously transported by more than one active motors[11]. Of the thirty beads that we tested that didn't interact with microtubules within the first 30 sec wait time, only one bound and moved after the first 30 sec. The resulting 2.5 % increase in overall binding fraction measured using 30 *vs.* 120 sec wait time is within the 7 % measurement error ($\sqrt{[p(1-p)/n]}$, where p is the measured binding fraction, n is the number of trial beads[11]). Taken together, binding fraction measurements are sufficient to detect the presence of the active, untreated motor(s) on the bead. An increase in binding fraction thus necessarily reflects an increase in the number of active motors on the bead, rather than an increase in the microtubule association rate of the active kinesin.

Kinetic calculation for equilibrium microtubule-kinesin association at 4 mM AMPPNP.

The dissociation constant, K_d, for the kinesin-microtubule interaction in the presence of 1 mM AMPPNP has been measured by Crevel, Lockhart, and Cross[29] to be 0.27±0.15 μM. Since the microtubule concentration (5 μM) in our microtubule pelleting assay was in significant excess than our kinesin concentration (~7.5 nM), we can estimate that

$$\frac{[Kin{\bullet}MT]_{eq}}{[Kin]_{tot}} = \frac{[MT]_{tot}}{K_d + [MT]_{tot}} \approx \frac{5}{0.27\mu M + 5\mu M} = 0.948,$$

where $[Kin{\bullet}MT]_{eq}$ is the concentration of kinesin bound to microtubules at equilibrium, $[Kin]_{tot}$ is the total concentration of active kinesin, and $[MT]_{tot}$ is the total concentration of tubulin-heterodimer. This equilibrium kinetic calculation suggests that 94.8% of all kinesins that are active ought to co-sediment with microtubule pellet at 4 mM AMPPNP. Thus microtubule pull-down assays provides a direct read out for the amount of active motors present.

Assuming that the entire motor population is active (as was assumed for these calculations), any potential effect of CK2 to increase kinesin's on rate, or decrease kinesin's off-rate, cannot result in a significant increase in kinesin binding to microtubules under our assay conditions (with 4 mM AMPPNP present). For example, a 100-fold increase in K_{on} could only increase the kinesin bound to microtubules from 94.8% to 99.9% of the total active population.

Time scale for the tail-independent inactivation/reactivation of K560.

To approximate the rate of tail-independent kinesin inactivation, we carried out microtubule pulldown assays of microtubule affinity purified K560 as rapidly as experimentally allowed for (Fig. 2d): within four hours of ATP release from the microtubule (Fig. 2b), and without any freeze-thaw cycles. This freshly purified K560 was placed on ice for 2.5 hours while we determined the motor concentration using Coomassie stained SDS-PAGE gel and BSA standards, and was then incubated with or without CK2 (3:1 CK2:K560 molar ratio) on ice for 1.5 hrs, followed by microtubule pulldown assays. More than half of the initially active K560 became incapable of binding/interacting with microtubule within four hours of the final purification step (ATP-release from microtubules), despite being kept on ice. CK2 increased the fraction of microtubule-bound K560 from the untreated 45 ± 6 % to 78 ± 5 % (mean ± SEM, n = 3, Fig. 2d). We were experimentally limited by the time necessary to assay for motor

concentration and the CK2-treatment. The tail-independent inhibition (and CK2-mediated activation) identified in this study, may occur more rapidly than the 4 hr (and 1.5 hr) reported here.

Supplementary Methods

Motor-bead association

Kinesin was first incubated with CK2 *in vitro* (26μL containing 75nM native kinesin or K560, 0nM or 250nM CK2, 30°C for 40min), then incubated with carboxylated polystyrene beads (0.5μm, Polysciences) at 160:1 beads:motor ratio in 80mM Pipes (pH6.9, 70μL total volume) for15 min at RT, followed by centrifugation at 2,000g for 15 min at 4°C. Bead pellets were washed thrice (80mM Pipes pH6.9, 70μL), boiled in 30μL 1x reducing SDS sample buffer for 15 minutes, and then centrifuged at 16,000g for 10 minutes at 4°C. Elute was separated by SDS-PAGE, analyzed by immunoblot or sypro stain (Invitrogen).

Liquid chromatography-mass spectrometry

K560 samples were subjected to *in vitro* CK2-treatment (0.5μg kinesin per 250U CK2, 30°C for 40 min), then reduced with 2mM DTT at 65°C for 30 min, alkylated with 15mM chloroacetamide in the dark at RT for 30 min, and quenched using 15mM cystine at RT for 30 min. Proteins were digested with trypsin at 37°C overnight. The tryptic digests were desalted off-line using Vivapure C18 micro spin columns (Vivascience) prior to LC–MS/MS. LC-MS/MS[45] was carried out by nanoLC system (Eksigent, Inc.) coupled with Linear Ion Trap (LTQ)-Orbitrap XL mass spectrometer (Thermo-Electron Corp).

Monoisotopic masses of parent ions and corresponding fragment ions, parent ion charge states and ion intensities from LC-MS/MS spectra were extracted using in-house software based on Raw_Extract script from Xcalibur v2.4. Following automated data extraction, the resultant peak lists for each LC-MS/MS experiment were submitted to the development version (5.0.0) of Protein Prospector (UCSF)

for database searching using a Swiss-Prot database (11/07/2007, 574100 sequence entries). *Homo sapien* was selected as the restricted species. Trypsin was set as the enzyme with a maximum of two missed cleavage sites. Chemical modifications such as protein N-terminal acetylation, methionine oxidation, N-terminal pyroglutamine, and deamidation of asparagine were selected as variable modifications. Since cysteine was reduced and alkylated, carbamidomethylation was chosen as a fixed modification. To map phosphorylation sites, phosphorylation of serine and threonine were chosen as variable modifications. The mass errors for parent ions were set as +/- 20ppm and for fragment ions as +/- 0.8Da. Search Compare program in Protein Prospector was used for summarization, validation, and comparison of results.

Gel filtration

500μg Ni-purified K560 (expressed in Terrific Broth for scaled-up protein production[46], zero freeze-thaw cycle) was analyzed using a Superdex-200 gel filtration column (Amersham Biosciences) in buffer A (50mM sodium phosphate pH8.0, 100mM NaCl), supplemented with 1mM DTT.

Dialysis

Ni-purified K560[46] (one freeze-thaw cycle) was dialyzed using Thermo Scientific Slide-A-Lyzer MINI Dialysis Unit (20K MWCO), for two hours on stir plate at 4°C. Dialysis buffer (80mM Pipes pH7.0, 5mM EDTA) was exchanged thrice (1L each, 40 min interval) for each dialysis.

Co-immunoprecipitation

K560 was first incubated with CK2 *in vitro* (20μL containing 75nM motor, 0nM or 65nM CK2 holoenzyme or subunits, 0°C for 1.5hr), then incubated with 50μL μMACS microbeads (Miltenyi Biotec) at 0°C for 30min. For immunoprecipitatation against the motor's C terminal His-tag, we used μMACS anti-His microbeads. For immunoprecipitation against kinesin's heavy chain, we used μMACS protein A microbeads, and preincubated 50μL protein A microbeads each with 2μg of SUK4 at 0°C for 30min before mixing with protein samples. Protein/microbeads mixture was washed in four

times in 200μL each of ice cold RIPA buffer (50mM TrisHCl pH8, 150mM NaCl, 1% NP-40, 0.5% $C_{24}H_{39}O_4Na$, 0.1% SDS), then rinsed in 100μL of ice cold low salt wash buffer (20mM TrisHCl pH7.5), and incubated with 20μL of 95°C elution buffer (50mM TrisHCl pH6.8, 50mM DTT, 1% SDS, 1mM EDTA, 0.005% bromphenol blue and 10% glycerol) for 5min at RT. Proteins were eluted with an additional 50μL of 95°C elution buffer. Elutes were separated by SDS-PAGE, analyzed by immunoblot.

Immunofluorescence imaging

Cos-1 cells were fixed (4% paraformaldehyde, 10 min at RT), permeabilized (2mg/ml BSA, 0.2% Triton X-100in PBS, 10 min on ice), blocked (3% BSA, 0.02% TritonX100 in PBS, 30 min at RT), and stained with primary (SUK4 or CK2α, 1:100 in blocking buffer for 1 hr at RT) followed by addition of Alexa Fluor conjugated secondary antibodies (488nm and/or 546/610nm, goat anti-mouse and/or goat anti-rabbit IgG; Invitrogen; 1:100 in blocking buffer for 1hr at RT), and imaged using LSM 510 confocal microscope or TIRF.

To quantify potential KHC/CK2α colocalization in Cos-1 cytosol, we used DAPI-stained images to generate masks for nuclei, and the JACoP plugin[47-48] (utilizing both intensity correlation and object-based colocalization coefficients) in ImageJ to analyze the nuclei-masked fluorescence images of KHC and CK2α.

Supplementary References

44 Leduc, C. *et al.* Cooperative extraction of membrane nanotubes by molecular motors. *Proc Natl Acad Sci U S A* **101**, 17096-17101 (2004).

45 Kaake, R. M., Milenkovic, T., Przulj, N., Kaiser, P. & Huang, L. Characterization of cell cycle specific protein interaction networks of the yeast 26S proteasome complex by the QTAX strategy. *J Proteome Res* **9**, 2016-2029 (2010).

46 Brodsky, O. & Cronin, C. N. Economical parallel protein expression screening and scale-up in Escherichia coli. *J Struct Funct Genomics* **7**, 101-108 (2006).

47 Manders, E. M. M., Verbeek, F. J. & Aten, J. A. Measurement of co-localization of objects in dual-colour confocal images. *J Microsc* **169**, 375-382 (1993).

48 Bolte, S. & Cordelieres, F. P. A guided tour into subcellular colocalization analysis in light microscopy. *J Microsc* **224**, 213-232 (2006).